

# Global Dynamic Molecular Profiling of Stomatal Lineage Cell Development by Single-Cell RNA Sequencing

Zhixin Liu<sup>1,4</sup>, Yaping Zhou<sup>1,4</sup>, Jinggong Guo<sup>1,4</sup>, Jiaoai Li<sup>2,4</sup>, Zixia Tian<sup>1</sup>, Zhinan Zhu<sup>1</sup>, Jiajing Wang<sup>1</sup>, Rui Wu<sup>1</sup>, Bo Zhang<sup>1</sup>, Yongjian Hu<sup>2</sup>, Yijing Sun<sup>2</sup>, Yan Shangguan<sup>2</sup>, Weiqiang Li<sup>1</sup>, Tao Li<sup>2</sup>, Yunhe Hu<sup>2</sup>, Chenxi Guo<sup>1</sup>, Jean-David Rochaix<sup>3</sup>, Yuchen Miao<sup>1</sup> and Xuwu Sun<sup>1,2,\*</sup>

<sup>1</sup>State Key Laboratory of Crop Stress Adaptation and Improvement, State Key Laboratory of Cotton Biology, Key Laboratory of Plant Stress Biology, School of Life Sciences, Henan University, 85 Minglun Street, Kaifeng 475001, China

<sup>2</sup>College of Life Sciences, Shanghai Normal University, Guilin Road 100, Shanghai, 200234, China

<sup>3</sup>Departments of Molecular Biology and Plant Biology, University of Geneva, Geneva, 1211, Switzerland

<sup>4</sup>These authors contributed equally to this article.

\*Correspondence: Xuwu Sun (sunxuwussd@sina.com)

<https://doi.org/10.1016/j.molp.2020.06.010>

## ABSTRACT

The regulation of stomatal lineage cell development has been extensively investigated. However, a comprehensive characterization of this biological process based on single-cell transcriptome analysis has not yet been reported. In this study, we performed RNA sequencing on 12 844 individual cells from the cotyledons of 5-day-old *Arabidopsis* seedlings. We identified 11 cell clusters corresponding mostly to cells at specific stomatal developmental stages using a series of marker genes. Comparative analysis of genes with the highest variable expression among these cell clusters revealed transcriptional networks that regulate development from meristemoid mother cells to guard mother cells. Examination of the developmental dynamics of marker genes via pseudo-time analysis revealed potential interactions between these genes. Collectively, our study opens the door for understanding how the identified novel marker genes participate in the regulation of stomatal lineage cell development.

**Keywords:** molecular profiling, stomatal, development, single-cell, RNA-seq

Liu Z., Zhou Y., Guo J., Li J., Tian Z., Zhu Z., Wang J., Wu R., Zhang B., Hu Y., Sun Y., Shangguan Y., Li W., Li T., Hu Y., Guo C., Rochaix J.-D., Miao Y., and Sun X. (2020). Global Dynamic Molecular Profiling of Stomatal Lineage Cell Development by Single-Cell RNA Sequencing. Mol. Plant. **13**, 1178–1193.

## INTRODUCTION

Stomata, which are formed by paired guard cells, have played crucial roles in the colonization of land by plants (von Groll and Altmann, 2001). Turgor-driven stomatal movement requires ion and water exchange with neighboring cells and controls transpiration and gas exchange between plants and the environment. To ensure efficient function, the development of stomata follows a one-cell-spacing rule, in which two stomata are separated by at least one non-stomatal cell (Bergmann and Sack, 2007; Pillitteri and Torii, 2012). In *Arabidopsis*, stomata develop from protodermal cells through a series of asymmetrical and symmetrical divisions (Han and Torii, 2016). At the beginning of stomatal development, a subset of protodermal cells becomes meristemoid mother cells (MMCs) by stochastically acquiring the stomatal progenitor cell fate (Qu et al., 2017). Through asymmetric divisions, meristemoids (Ms) and stomatal lineage ground cells (SLGCs) are produced from MMCs (Qu et al.,

2017). Ms can further differentiate directly into guard mother cells (GMCs) or undergo several rounds of amplifying divisions, while SLGCs might reacquire the MMC fate and undergo spacing divisions or differentiate into a pavement cell (PC) (Rudall et al., 2013; Qu et al., 2017). Finally, GMCs can divide symmetrically to produce a pair of guard cells (GCs) (Geisler et al., 2000). Divisions of M cells result in the final spacing between stomata (Pillitteri and Torii, 2012).

Several key genes and regulatory networks underlying stomatal development have been uncovered by molecular and genetic analyses. The closely related basic helix-loop-helix (bHLH) transcription factors (TFs) SPEECHLESS (SPCH), MUTE, and FAMA control sequential cell fate transitions from MMC to M, M to

GMC, and GMC to GC, respectively (Ohashi-Ito and Bergmann, 2006; MacAlister et al., 2007; Pillitteri et al., 2007). The expression profiles of these TFs are also specifically associated with different stomata developmental stages. For example, the GFP signals of *SPCHpro::nucGFP* and *SPCHpro::SPCH-GFP* can be detected in a subset of epidermal cells that lack overt signs of differentiation (MacAlister et al., 2007). *MUTE* is required to limit the number of rounds of M divisions and is expressed strongly in Ms and at lower levels in GMCs and GCs (Pillitteri et al., 2007). *FAMA* is expressed in GMCs and is necessary and sufficient to promote GC identity (Ohashi-Ito and Bergmann, 2006). *FAMAPro::GFP* is not expressed in Ms but is strongly expressed in GMCs and young guard cells (YGCs) (Ohashi-Ito and Bergmann, 2006). To specify each cell-differentiation state, SPCH, MUTE, and FAMA form heterodimers with two paralogous bHLH-leucine zipper (bHLH-LZ) TFs, SCREAM (SCRM) and SCRM2 (Kanaoka et al., 2008). In addition, two partially redundant R2R3 MYB TFs, FOUR LIPS (FLP) and MYB88, control stomatal terminal differentiation independently of FAMA (Lai et al., 2005; Ohashi-Ito and Bergmann, 2006).

Two secreted cysteine-rich peptides, EPIDERMAL PATTERNING FACTOR1 (EPF1) and EPF2, are expressed at later and earlier stages of stomatal development, respectively. EPF2 is produced in MMCs, whereas EPF1 is produced in late-stage Ms, GMCs and YGCs (Hara et al., 2007; Hunt and Gray, 2009a). These peptides are perceived by cell-surface receptors, the ERECTA (ER)-family leucine-rich repeat receptor kinases ER-LIKE1 (ERL1) and ERL2, resulting in inhibition of stomatal development (Shpak et al., 2005; Hara et al., 2007; Hunt and Gray, 2009b; Lee et al., 2012). The receptor-like protein TOO MANY MOUTHS (TMM) modulates the signaling strength of ER-family receptor kinases in a domain-specific manner (Nadeau and Sack, 2002; Lee et al., 2012). *TMMpro::TMM-GFP* is expressed in proliferating stomatal lineage cells, but not in other epidermal cells or in mature stomata (Nadeau and Sack, 2002). The transcript levels of *TMM* in *scrm-D mute*, which only produces Ms, is significantly higher than in wild type (WT) (Pillitteri et al., 2011). The expression of *TMM* is also high in MMCs (Pillitteri et al., 2007; Adrian et al., 2015). Expression of HIGH CARBON DIOXIDE (H/C), which encodes 3-ketoacyl-CoA synthase 13 (KCS13), is highest in GCs (Gray et al., 2000). Genetic evidence suggests that these signals are mediated by a YODA (YDA)-mitogen-activated protein kinase (MAPK) cascade, which eventually downregulates the TFs responsible for initiating stomatal lineage development through direct phosphorylation (Bergmann et al., 2004; Lampard et al., 2008, 2009; Kim et al., 2012; Putarjunan et al., 2019; Samakovli et al., 2020; Xue et al., 2020). Samakovli et al. (2020) found that upstream of the YDA-MAPK module, HEAT SHOCK PROTEINS 90 (HSP90s) can interact with YDA and regulate its cellular polarization and the phosphorylation of downstream targets (e.g., MPK6 and SPCH) under both normal and heat-stress conditions. In addition, Xue et al. (2020) identified three plasma membrane-associated MAPK SUBSTRATES IN THE STOMATAL LINEAGE (MASS) proteins that can be phosphorylated by MPK3/6. On the plasma membrane, MASS interacts with YDA to directly or indirectly regulate MAPK signaling during stomatal development (Xue et al., 2020). A very recent report revealed that downstream of the YDA-MAPK module, an MAP Kinase Docking and KRAAM

(KiDoK) motif on SCRM is essential for binding MPK6 (Putarjunan et al., 2019). SCRM therefore functions as a scaffold and bridges MAPKs and SPCH to enforce entry into the stomatal lineage pathway (Putarjunan et al., 2019). The stomagen (also known as EPF-LIKE9) peptide promotes stomatal development by competing with EPF2 for binding to ER (Sugano et al., 2010; Zhang et al., 2014; Hronkova et al., 2015).

Peterson et al. (2013) reported that one homeodomain-leucine zipper IV (HD-ZIP IV) protein, HOMEO DOMAIN GLABROUS2 (HDG2), acts as a key epidermal component promoting stomatal differentiation. The *hdg2* mutant exhibits delayed M-to-GMC transition (Peterson et al., 2013). Further analysis of the expression of a HDG2 transcriptional reporter (*HDG2pro::nls-3xGFP*) and a translational reporter (*HDG2pro::HDG2-GFP*) indicated that not only the transcript but also the HDG2 protein are strongly expressed in Ms and SLGCs (Peterson et al., 2013). Although these results suggest that *HDG2* is specifically expressed in Ms, and the expression of *HDG2* is strongly increased in *scrm-D mute*, which produces an epidermis solely composed of Ms and SLGCs (Pillitteri et al., 2011), the highest enrichment of *HDG2* transcripts is found in MMCs, rather than in Ms (Supplemental Figures 4A and 6B).

MMCs can produce Ms and SLGCs through asymmetric cell divisions regulated by BASL and POLAR (Dong et al., 2009; Houbaert et al., 2018). In the cotyledon and leaf epidermis, *BASL::GUS* is highly expressed in the asymmetrically dividing MMCs and Ms and is undetectable in later stomatal lineage cells (Dong et al., 2009). Further investigations revealed that BASL and POLAR show largely overlapping localization at the cell cortex during stomatal asymmetric divisions and can directly interact with each other (Houbaert et al., 2018). In addition to stomatal lineage cells, PCs are also produced from MMCs and are important components of the epidermis. However, the identification of PCs is relatively difficult due to the lack of specific marker genes. *ML1pro::YFP-RCI2A* was used as marker gene for identifying the entire aerial epidermis (Adrian et al., 2015). The available evidence indicates that microtubule-associated protein IQ67 DOMAIN 5 (IQD5) is localized in PCs (Liang et al., 2018). *GFP::IQD5* co-localizes with the microtubule marker *mCherry::TUB6* (*mCherry* fused to  $\beta$ -tubulin6) in both leaf PCs and hypocotyl epidermal cells (Liang et al., 2018). One important feature of PCs is that they contain chloroplasts, which require the expression of photosynthesis-related genes (Barton et al., 2016). These features need to be considered for the identification of PCs.

The transcriptome dynamics of stomatal lineage cells has been characterized by isolating stomatal lineage cells with fluorescence-activated cell sorting (FACS) (Adrian et al., 2015). Transcriptome analysis of isolated protoplasts of GCs and mesophyll cells (MPCs) has been used to investigate the response of GCs and MPCs to abscisic acid treatment (Yang et al., 2008). These results suggest that isolated protoplasts can be used to investigate the transcriptome profiles of stomatal lineage cells. However, gene expression profiles for different types of stomatal lineage cells at the single-cell level are currently lacking, resulting in a poor understanding of the regulatory mechanisms controlling the development of these

cells. To gain new insights into these processes, we isolated protoplasts from cotyledons of 5-day-old *Arabidopsis* seedlings for single-cell RNA sequencing (scRNA-seq). We classified the major cell types and employed transcriptomic analysis to identify several potential key regulators present in these heterogeneous cell populations. Our analysis led to the identification of a regulatory network of TFs for specific developmental stages from MMCs to GMCs. Pseudo-time analysis was employed to uncover the interactions and mutual regulation among key marker genes. We also identified several novel marker genes that play important roles in regulating stomatal development. These results provide insights into how single-cell transcriptomics can be used to further elucidate the regulatory mechanisms controlling the differentiation of stomatal lineage cells.

## RESULTS

### Gene Expression Patterns in Stomatal Lineage Cells

To systematically resolve gene expression patterns in specific stomatal lineage cells at different developmental stages, we prepared protoplasts by enzymatic digestion of cotyledons of 5-day-old seedlings. Identification of specific cell types from isolated protoplasts of whole tissue using marker genes has been successfully used by several groups to investigate the profiles of root cells (Denyer et al., 2019; Jean-Baptiste et al., 2019; Ryu et al., 2019; Zhang et al., 2019). Protoplasts were screened through a 40- $\mu$ m pore cell strainer to obtain more than 20 000 individual cells. Single cells were labeled using 10X Genomics barcode technology, followed by reverse transcription to obtain a single-cell cDNA library (Supplemental Figure 1). This cDNA library was utilized for high-throughput sequencing (Supplemental Figure 1). After extensive analysis of the sequencing results, we obtained transcriptome information for 13 999 single cells (Supplemental Figure 2). We also identified mitochondrial (mito), chloroplast (pt), and ribosomal (ribo) transcriptomes. A strong correlation (Pearson's  $r = 0.64$ ,  $p < 2.2e-16$ ) between gene expression levels from RNA-seq of bulk pooled cotyledons of 5-day-old seedlings and the average gene expression levels from RNA-seq of single cells indicated that the quality of the scRNA-seq data was high (Supplemental Figure 2F). Transcripts from the subcellular organelles were excluded from subsequent analysis, resulting in 12 844 single-cell transcriptomes that were further analyzed. Cells were classified into 11 clusters using t-distributed stochastic neighborhood embedding (tSNE) (Figure 1A and Supplemental Table 1). The percentage of cells in each cluster ranged from 2.2% to 22.4% (Figure 1B). It is worth mentioning that the percentage for each cell type only represents percentage of cells harvested in this study, and therefore does not reflect the actual cell proportion in cotyledons. To check whether different dimensional reduction techniques give rise to similar stomatal cell clusters, we used the uniform manifold approximation and projection (UMAP) algorithm to visualize the cell clusters (Supplemental Figure 3A and Supplemental Table 2). Similar cell clusters were identified with UMAP (Supplemental Figure 3A). In addition, Pearson's correlation analysis was performed and the results indicated that the cell clusters identified by tSNE and UMAP are highly correlated (Supplemental Figure 3B). As shown in Supplemental Figure 3C, some marker genes identified by tSNE were also identified by UMAP. These results indicate that different dimensional reduction techniques yield similar cell clusters.

Because expression of some marker genes occurs at different stomata developmental stages in variable amounts, we used more than one marker gene to identify the cell types representative of the different stages of stomata development. For MPCs, we used *Ribulose Bisphosphate Carboxylase Small Subunit* (*RBCS*) and *light-harvesting chlorophyll a/b-binding protein* as markers; these genes encode chloroplast proteins that are highly expressed in MPCs (Salesse et al., 2017; Liu et al., 2020). With respect to the epidermal cell population, we selected *HDG2*, *POLAR*, *SPCH*, *TMM*, *MUTE*, and *EPF2* for MMCs (Pillitteri et al., 2007, 2011; Pillitteri and Dong, 2013; Adrian et al., 2015; Yang et al., 2015); *MUTE*, *BASL*, *SPCH*, and *EPF2* for early-stage meristemoid (EM) cells (Pillitteri et al., 2007; Pillitteri and Dong, 2013; Yang et al., 2015); *BASL*, *MUTE*, and *EPF1* for late-stage meristemoid (LM) cells; *EPF1*, *HIC*, *FAMA*, and *SCRM* for GMCs (Pillitteri and Dong, 2013; Adrian et al., 2015); and *RBCS*, *FAMA*, and *EPF1* for YGCs (Hara et al., 2007; Pillitteri and Dong, 2013; Adrian et al., 2015). High expression of *RBCS*, *FAMA*, and *SCRM* combined with low expression of *TMM* was used as a marker for GCs (Gray et al., 2000; Hara et al., 2007; Pillitteri et al., 2007; Pillitteri and Dong, 2013), and *IQD5* and *RBCS* expression as a marker for PCs (Barton et al., 2016; Liang et al., 2018). Because there are chloroplasts in GCs and YGCs, we also used *RBCS* as a marker for these cells (Barton et al., 2016; Salesse et al., 2017). The diagrams in Figure 1C and 1D display the expression patterns of selected marker genes in different stomatal cell types.

### Identification of Cell Types with Marker Genes

To determine the cell type using the aforementioned marker genes, we analyzed the pattern of selected marker genes in each cell cluster. As shown in Supplemental Figure 4A, *SPCH* expression is high in cluster 8; *MUTE* is expressed in clusters 8 and 10; while *FAMA*, *TMM*, *HIC*, and *SCRM* are expressed in clusters 7 and 10. High expression of *POLAR* is found in cluster 8, while *BASL* is highly expressed in cluster 10 (Supplemental Figure 4A). *EPF1* is expressed in cluster 10, while *EPF2* is expressed in clusters 8 and 10 (Supplemental Figure 4A). *RBCS* and *IQD5* are highly expressed in cluster 0, where the expression of stomata marker genes is very low (Supplemental Figure 4A). The feature plots of the selected marker genes show expression profiles similar to those of the heatmap (Supplemental Figure 4A and 4B). For instance, expression of *FAMA*, *TMM*, *HIC*, and *SCRM* is mainly enriched in clusters 7 and 10 (Supplemental Figure 4B). Based on the expression patterns of these marker genes, we can determine the cell type of each cluster as follows: cluster 0 is PC, cluster 8 is MMC, cluster 3 is EM, cluster 4 is LM, cluster 10 is GMC, cluster 7 is YGC, and cluster 6 is GC (Figure 1A). Expression of *RBCS* and *PSAB* is mainly enriched in clusters 2 and 5, indicating that these clusters correspond to MPCs. To distinguish them, we named them MPC\_2 and MPC\_5, respectively (Figure 1A). For cluster 1 and cluster 9, we could not determine the cell type using the known marker genes. However, for the genes that belong to cluster 9, we checked the stomatal pattern in the corresponding mutants. As an example, we found that the SI (stomatal index) of *BCL-2-ASSOCIATED ATHANOGENE 6* (*bag6*) was higher

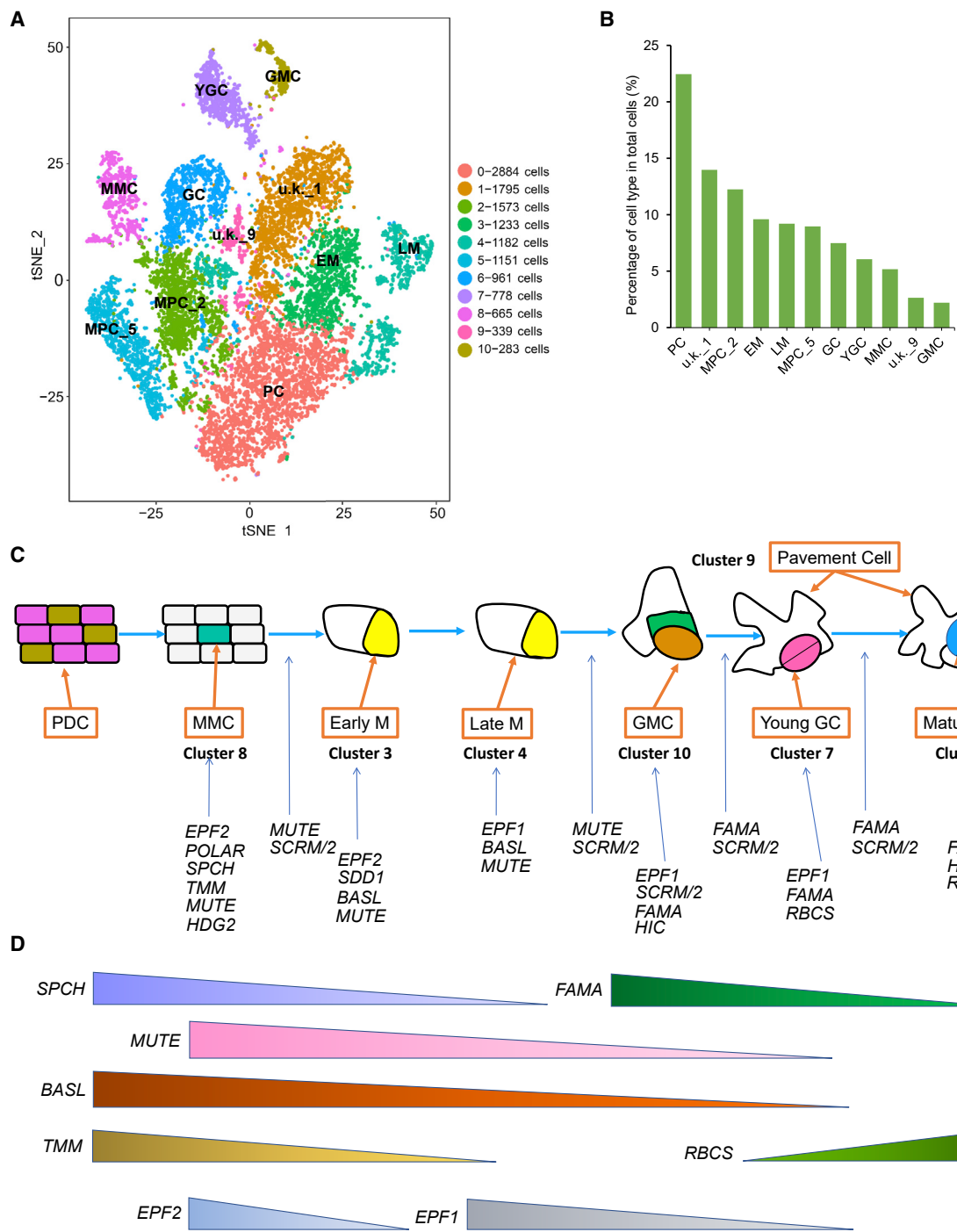


**Figure 1. Identification of Cell Types with Representative Marker Genes.**

(A) Identification of cell types according to the expression pattern of marker genes in each cell cluster. PC, pavement cell; GMC, guard mother cell; GC, guard cell; MMC, meristemoid mother cell; EM, early-stage meristemoid; LM, late-stage meristemoid; YGC, young guard cell; MPC, mesophyll cell; u.k., unknown.

(B) Relative abundance of each cell type expressed as a percentage of the whole population of cells used in this study.

(C) Diagram of expression of marker genes in different cell types.

(D) Illustration of the dynamic pattern of marker gene expression during development of stomata.

compared with WT (Supplemental Figure 5A and 5B). However, stomata development in another mutant of one of the marker genes of cluster 9, *bzip6*, was not significantly affected.

#### Expression of Marker Genes in Stomatal Lineage Cells

To further test the cell types that we identified, we analyzed the expression of several known marker genes that are involved in regulating the development of stomatal lineage cells. As shown

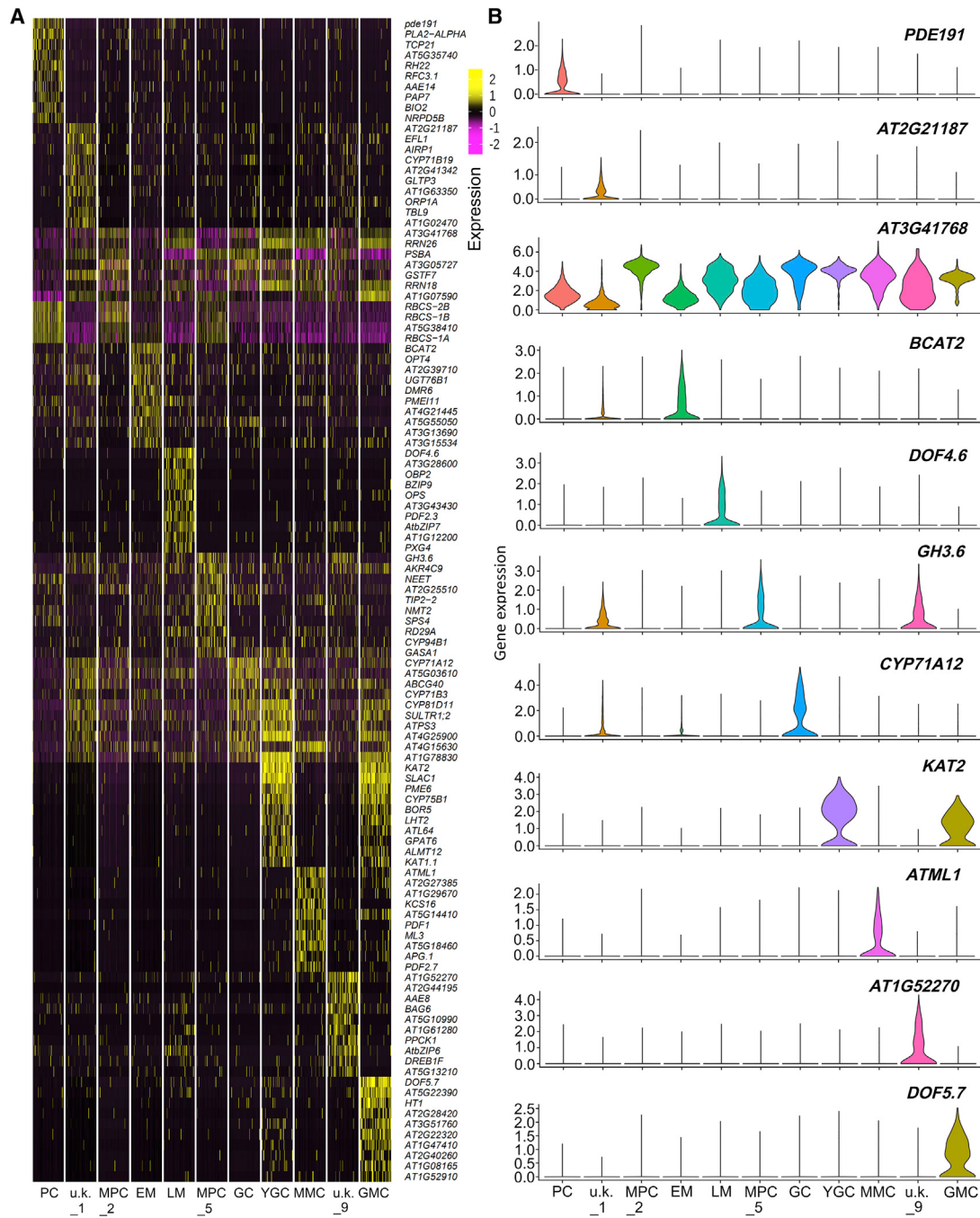
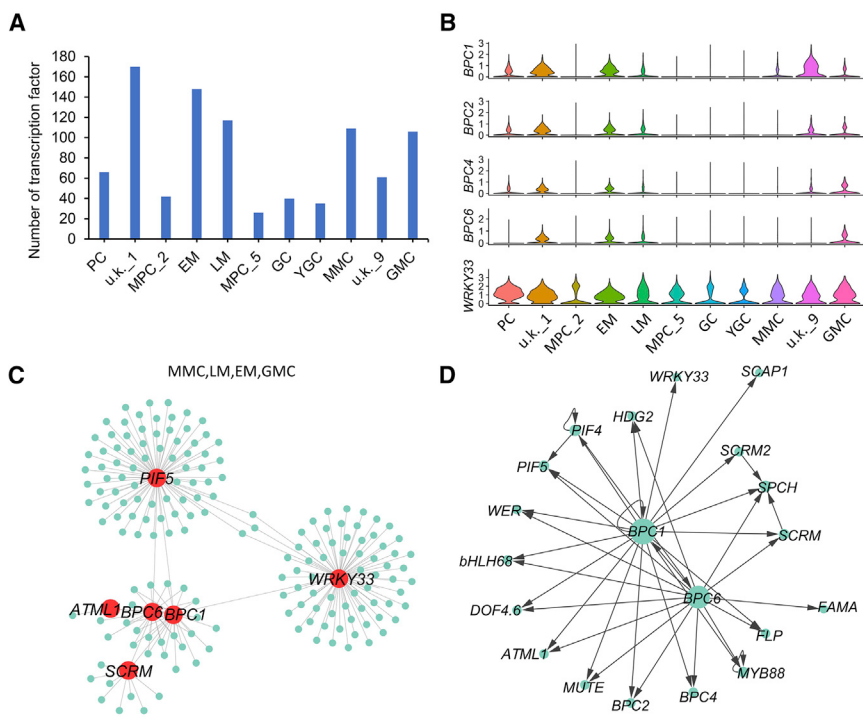


**Figure 2. Identification of Novel Marker Genes for Each Cluster.**

(A) Heatmap of expression levels of representative marker genes in each cluster.  
(B) Violin plots show expression levels of representative marker genes in each cell type.

in *Supplemental Figure 4B*, *FAMA*, *TMM*, *HIC*, and *SCRM* are specifically expressed in YGCs and GMCs, whereas the other marker genes are not specifically expressed in particular cell types (*Supplemental Figure 4B*). To explore the potential regulators of stomatal lineage cells, we analyzed gene expression profiles in different clusters and identified highly expressed marker genes in each individual cell cluster (*Figure 2A* and *2B*). Some of these marker genes could

potentially be involved in regulating the development of stomatal lineage cells, for example, *SLAC1* and *SCAP1* (*DOF5.7*) (Engineer et al., 2015; Chen et al., 2016). Consistent with the report that the pectin methylesterase gene 6 (*PME6*) is highly expressed in GCs and is required for stomatal function (Amsbury et al., 2016), our results indicate that *PME6* is highly expressed in YGCs and GMCs (*Figure 2A*). To verify the expression pattern of marker genes, we compared their



expression profiles in our study with those reported previously (Yang et al., 2008; Adrian et al., 2015). As shown in Supplemental Figure 6, consistent with the reported results of Adrian et al. (2015) and Yang et al. (2008), some marker genes show higher expression in stomatal lineage cells; for example, *ATML1* and *TMM* are highly expressed in GMCs and MMCs. However, the expression of some newly identified marker genes from our study showed different patterns from those of Adrian et al. (2015); for instance, the LM marker gene *bZIP* shows high expression in both LMs and GCs and the MMC marker gene *AT1G29670* also shows high expression in YGCs (Figure 2 and Supplemental Figure 6). The identification of PCs is relatively difficult due to the lack of specific marker genes. By comparing the epidermis marker genes identified by FACS with the reporter *ML1pro::YFP-RCI2A*, we found that the highest overlapping percentage (41%) of epidermis marker genes occurred with the enriched genes in PCs identified in this study (Supplemental Table 3). The SI of around 35% indicates that about 60% of the epidermis is composed of PCs (Lee et al., 2015). Therefore, these results indirectly support the identification of PCs in this study.

#### Gene Ontology Analysis of Genes Enriched in Different Cell Types

To investigate the potential biological functions of genes expressed in each cell type, we performed gene ontology (GO) analysis of all cell clusters (Supplemental Figures 7 and 8). In general, the majority of enriched terms were associated with individual cell types. Those GO terms associated with multiple cell types represented more general biological processes (e.g., response to oxidative stress and salt stress, and vesicle-mediated transport) (Supplemental Figures 7A and 8). As a measure of the reliability of the method for identifying cell-type-expressed genes and of the ability to correctly attribute biological

#### Figure 3. Identification of Regulatory Networks of Transcription Factors in Different Cell Types.

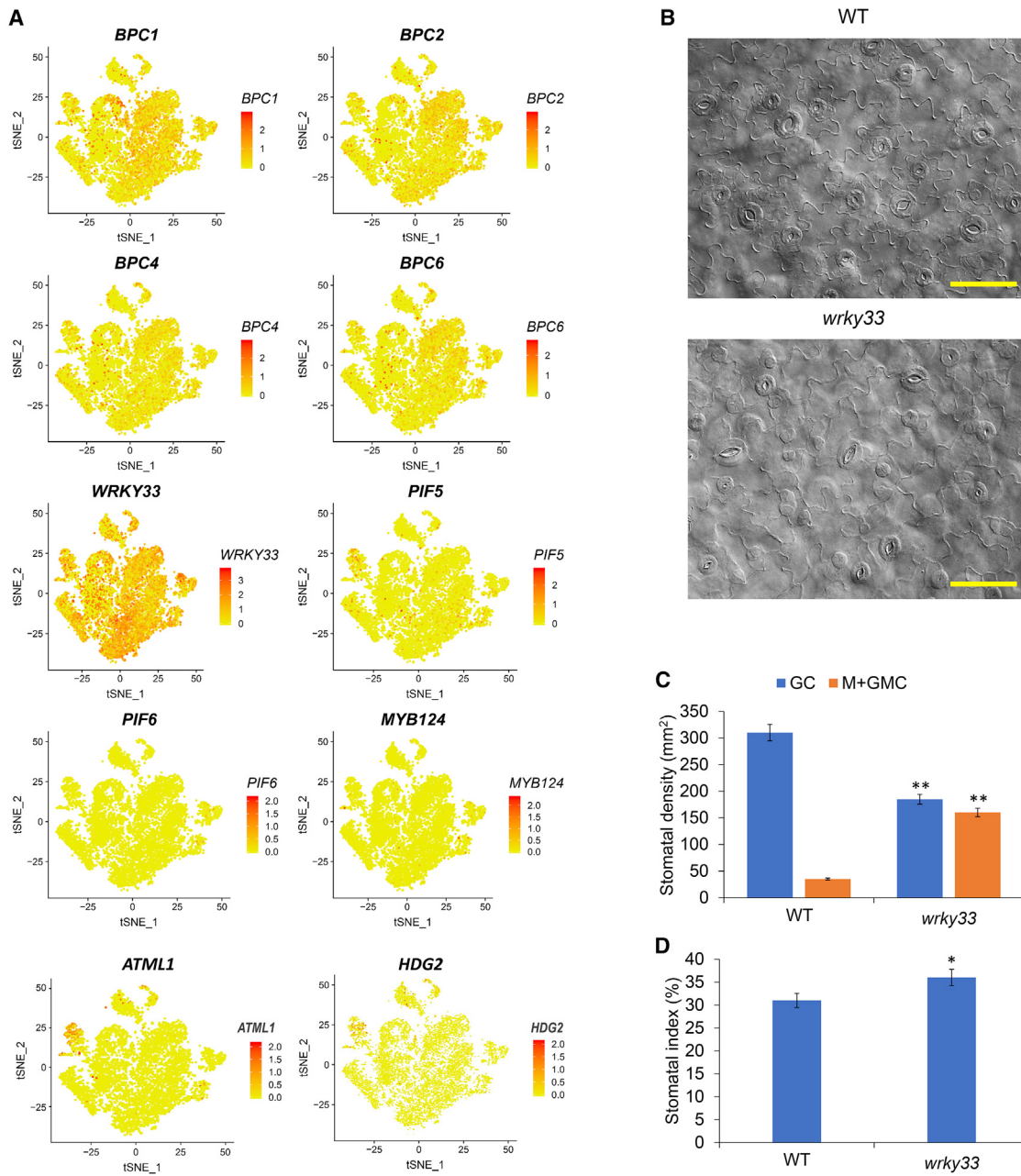
- (A) Identification of the transcription factors (TFs) in different cell types.
- (B) Violin plot of the expression levels of TFs identified in MMCs, EMs, and GMCs.
- (C) Analysis of the regulatory network of TFs identified in MMCs, EMs, LMs, and GMCs.
- (D) Analysis of the mutual regulation between known TFs and newly identified TFs.

processes to a cell type, we compared a list of genes enriched in GCs with genes identified in previous studies on GC functions. In agreement with the published reports (Gray, 2005; Lawson, 2009; Song et al., 2014; Niu et al., 2018; Huang et al., 2019), we found that genes responding to oxidative stress, salt stress, bacteria, and cadmium ions and that are involved in stomatal movement and photosynthesis are highly expressed in GCs and other stomatal lineage cells (Supplemental Figures 7A and 8). Our analysis further increased the spectrum of

biological processes associated with GC development to include protein transport and cell death (Supplemental Figures 7A and 8). GO heatmap analysis revealed that MMCs, EMs, LMs, and GMCs are similar (Supplemental Figure 7A and 7B). In these cells, the expressed genes are not involved in photosynthesis (Supplemental Figure 7A). However, genes enriched in EMs and GMCs are implicated in protein transport and vesicle-mediated transport (Supplemental Figures 7A and 8).

#### Analysis of the Regulatory Network of Transcription Factors in Early Development of Stomatal Lineage Cells

To discover the potential TFs that are involved in regulating the early development of stomatal lineage cells, we surveyed the TFs that show high expression in different cell types. The highest number of TFs was identified in unknown (u.k.)\_1 while the lowest number was identified in MPC\_5 (Figure 3A). Interestingly, we found that the expression of *BASIC PENTACysteine 1* (*BPC1*), *BPC2*, *BPC4*, *BPC6*, and *WRKY33* is significantly higher in MMCs, EMs, and GMCs (Figure 3B). BPC proteins and WRKY33 are important TFs involved in regulating growth and development and the stress response of seedlings (Monfared et al., 2011; Wang et al., 2018; Schmidt et al., 2020). To investigate the mechanisms by which BPCs and WRKY33 regulate the early development of stomatal lineage cells, we analyzed the regulatory network in which they are involved in MMCs, EMs, LMs, and GMCs by analyzing the genes co-expressed with them and extracted the top 200 links showing positive correlation with the TFs. As shown in Figure 3C and Supplemental Table 4, *ATML1*, *BPC1*, *BPC6*, *SCRM*, *PIF5*, and *WRKY33* may act as core TFs to regulate the expression of target genes in MMCs, EMs, LMs, and GMCs. To investigate the mutual regulation between BPCs and WRKY33 and known TFs, we analyzed their regulatory

**Figure 4. Analysis of Feature Plots and Functions of Core TFs.**

(A) Feature plots of the expression of representative TFs in different clusters.

(B) Developmental pattern of stomatal lineage cells in cotyledons of 5-day-old seedlings of *wrky33*, with wild type (WT) used as control. Scale bars, 50  $\mu$ m.

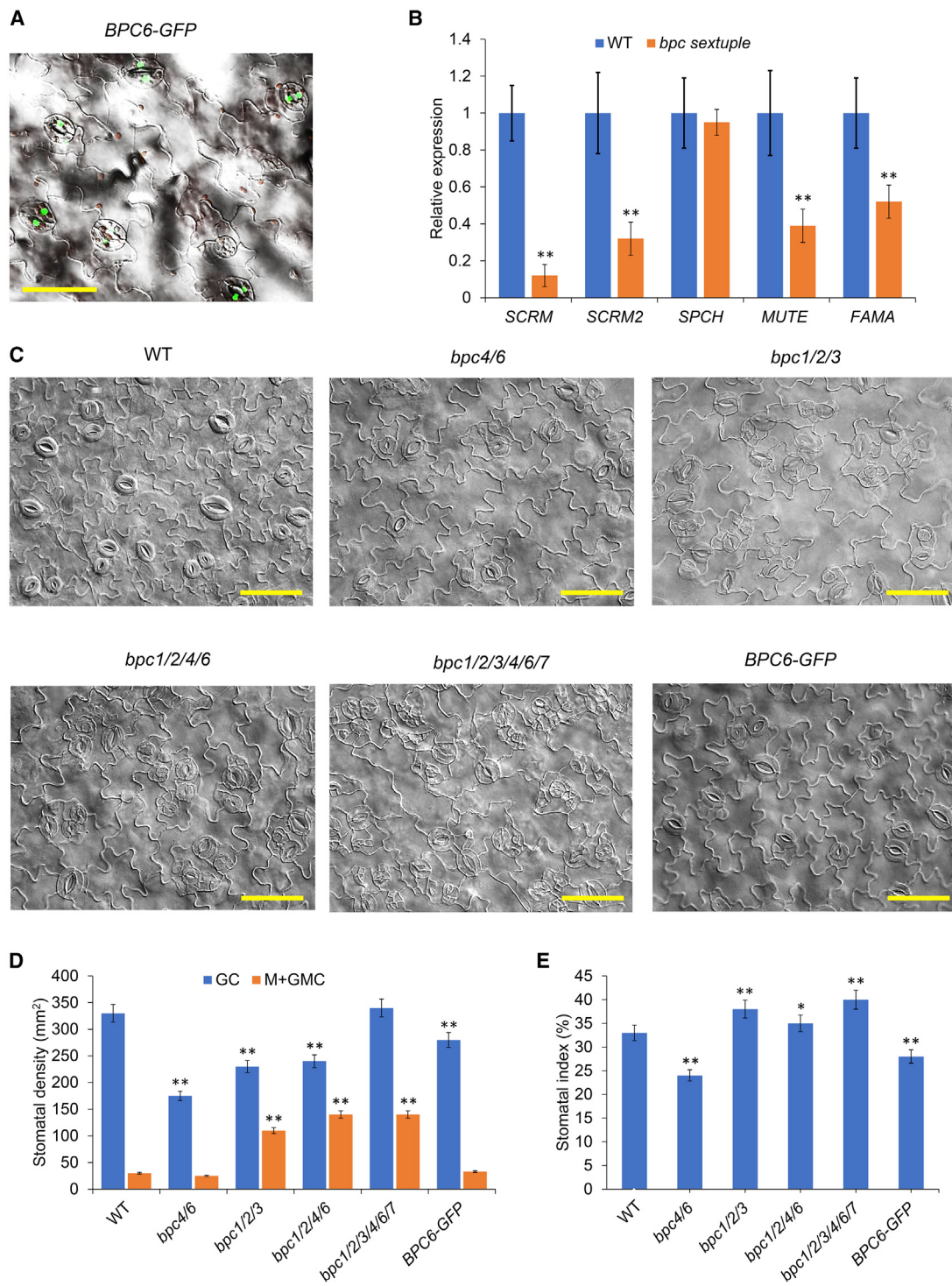
(C and D) Stomatal density (C) and stomatal index (D) of cell types calculated from (B). Error bars represent standard errors (SE). \* $p$  < 0.05, \*\* $p$  < 0.01, Student's *t*-test analysis versus WT.

network. As shown in Figure 3D, BPC1 and BPC6 positively regulate most known TFs based on co-expression, suggesting that BPC1 and BPC6 may regulate early stomatal lineage cell development through these interactions.

#### WRKY33 and BPCs Are Involved in Regulating the Early-Stage Development of Stomata

To investigate the effects of identified TFs on the development of stomatal lineage cells, we analyzed their expression feature plots.

As shown in Figure 4A, the expression of *BPC1*, *BPC2*, *BPC4*, and *BPC6* is mainly enhanced in MMCs, EMs, and GMCs, while the expression of *WRKY33* can be detected in all cell types (Figure 4A). Analysis of the stomatal developmental pattern indicated that the number of GCs is lower while the numbers of Ms and GMCs are higher in *wrky33* compared with WT (Figure 4B–4D), suggesting that *wrky33* is also defective in the regulation of differentiation of cells from Ms to GMCs or GMCs to GCs. BPC6 has been shown to participate in the regulation of *ABI4* (Mu et al., 2017), and our subcellular localization study

**Figure 5. BPC Proteins Are Involved in Regulating the Development of Stomata.**(A) Analysis of the subcellular localization of BPC6-GFP. Scale bar, 50  $\mu$ m.(B) qPCR analysis of the expression of marker genes in the *bpc* sextuple mutant.(C) Developmental patterns of stomatal lineage cells in cotyledons of 5-day-old seedlings of *bpc* mutants and transgenic plants; WT was used as control. Scale bars, 50  $\mu$ m.(D and E) Stomatal density (D) and stomatal index (E) calculated from (C). Error bars represent SE. \* $p$  < 0.05, \*\* $p$  < 0.01, Student's *t*-test analysis versus WT.

indicated that BPC6-GFP is localized in the nucleus of GCs (Figure 5A). Quantitative real-time PCR (qPCR) analysis indicated that the expression levels of *SPCH*, *MUTE*, *FAMA*, *SCRM*, and *SCRM2* are lower in the *bpc1 bpc2 bpc3 bpc4 bpc6 bpc7* sextuple mutant than in WT (Figure 5B). Further analysis showed that the SI was higher in the *bpc1 bpc2 bpc4 bpc6* quadruple mutant and the *bpc1 bpc2 bpc3 bpc4 bpc6 bpc7* sextuple mutant, whereas the SI was lower in *BPC6-GFP* compared with WT (Figure 5C–5E). Interestingly, there were more Ms and GMCs in the *bpc1 bpc2 bpc3* triple, *bpc1 bpc2 bpc4 bpc6* quadruple, and *bpc1 bpc2 bpc3 bpc4 bpc6 bpc7* sextuple mutant than in WT, but there were fewer GCs in these mutants than in WT, except for the *bpc1 bpc2 bpc3 bpc4 bpc6 bpc7* sextuple mutant, which had more GCs than the WT (Figure 5D). The observation that expression levels of *BPC1*, *BPC2*, *BPC4*, and *BPC6* are higher in EMs, LMs, and GMCs suggests that BPCs may mediate early stomatal development from Ms to GMCs.

### ATML1 Is Required for Regulating the Development of MMCs

To explore potential regulators of MMCs, we analyzed the marker genes in MMCs and found that *ATML1* displays an expression pattern highly similar to that of *HDG2* (Figure 4A), an important factor for regulating the differentiation from Ms to GMCs (Peterson et al., 2013). Previous studies showed that overexpression of *ATML1* induces stomata-like structures in the inner cells of cotyledons (Takada et al., 2013). These ectopic GC-like cells expressed the GC marker *KAT1-GUS*, suggesting that these cells have GC identity (Takada et al., 2013). Moreover, induction of *ATML1* repressed expression of the mesophyll-specific reporter *STOMAGEN-GUS* resulting in misshaped leaves with ectopic patches of transparent cells among the green mesophyll tissues (Takada et al., 2013). Also, the SI of the *atml1* mutant is lower while the SI of transgenic plants overexpressing *ATML1* is higher (Peterson et al., 2013), suggesting that *ATML1* is involved in regulating stomatal development. However, these previous reports did not demonstrate whether *ATML1* directly regulates the early development of stomata. To investigate whether *ATML1* can regulate the biogenesis of stomatal lineage cells, we isolated mutants of *ATML1*. As expected, *atml1-3* plants are deficient in the biogenesis of stomatal lineage cells, and the SI and stomatal density of *atml1-3* are lower than in WT (Supplemental Figure 9A–9D). Further qPCR analysis indicated that the expression levels of the key marker genes *SPCH* and *MUTE* in *atml1-3* were lower than in WT (Supplemental Figure 9E), suggesting that *ATML1* might regulate the biogenesis of stomatal lineage cells by modulating the expression of both *SPCH* and *MUTE*. Alternatively, the lower expression of *SPCH* and *MUTE* may result from the lower number of stomatal precursor cells in *atml1-3*.

### Developmental Pseudo-Time Analysis of Marker Gene Expression

To reconstruct the developmental trajectory during differentiation, we performed pseudo-temporal ordering of cells (pseudo-time analysis) based on our scRNA-seq data using Monocle 2 (Trapnell et al., 2014). The pseudo-time path has a total of three branches (Figure 6A and 6B), and different cell clusters are

arranged relatively clearly at different branch sites of the pseudo-time path (Figure 6B and Supplemental Figure 10). In general, the developmental processes of stomatal lineage cells are from MMCs to GCs (Figure 6B). Surprisingly, PCs were concentrated in a pseudo-time branch that was significantly different from that of the other cell types (Figure 6B and Supplemental Figure 10). Intriguingly, we found that MMCs and GMCs could not be clearly distinguished on the pseudo-time curve (Figure 6B and Supplemental Figure 10). In principle, the distribution characteristics of different cell types on the developmental trajectory can preliminarily determine the relationship between these cells during different developmental stages. The distribution of GMCs and YGCs in the development trajectory is relatively concentrated, but MPC\_2 and MPC\_5 can be found at several time points along the developmental trajectory (Figure 6B and Supplemental Figure 10), suggesting that the development of MPCs is more complex. Interestingly, we found that u.k.\_1 and EM show relatively similar distribution patterns in the developmental trajectory, suggesting that their developmental stages are similar. Although PCs are mainly distributed in branch 1 at the end stage of the development trajectory, they are also distributed at other time points.

To analyze the pseudo-time patterns of representative marker genes, we selected the top five marker genes in each cluster (Figure 6C). As shown in Figure 6C, the heatmap of pseudo-time for the top five marker genes shows that their pseudo-time patterns can be classified into two clusters (Figure 6C). In the first cluster, the expression of all the marker genes increases gradually along with pseudo-time (Figure 6C). In contrast, expression of marker genes in cluster 2 decreases at the end of the pseudo-time axis (Figure 6C). The marker genes in the first cluster are mainly from MPCs, suggesting that MPCs are at a more mature stage of development (Figure 6C). The second cluster can be divided into three branches: in the first branch, expression of marker genes mainly from YGCs, GCs, and MPCs first gradually increases to a maximum level and then decreases quickly along pseudo-time; in the second branch, expression of marker genes mainly from u.k.\_1 and EM is very high at the beginning of development but quickly decreases along pseudo-time; in the third branch, expression of the marker genes mainly from MMC and EM is lower during all of the developmental periods along pseudo-time and further declines at the last stage of pseudo-time (Figure 6C).

Expression of the marker genes *EPF1*, *SPCH*, and *MUTE* is highly similar at the early stages of development (Figure 7A and 7B). In particular, expression of *MUTE* is highest in MMCs but quickly decreases to a very low level, which is consistent with the expression pattern described by Pillitteri et al. (2007). As expected, *EPF2*, *FAMA*, and *SCRM* exhibit a similar pseudo-time pattern, which is consistent with the functional interactions between *FAMA* and *SCRM* during differentiation from GMCs to GCs (Figure 7A and 7B). Although *SCRM* and *SCRM2* have some functional interactions with *MUTE* and *SPCH* in the regulation of stomatal lineage cell development, our pseudo-time results show that expression of the *SCRM*, *SCRM2*, *MUTE*, and *SPCH* genes is significantly different (Figure 7A and 7B). Interestingly, our results show that *SPCH* displays a pattern similar to that of *ERL1*, *EPF1*, and *HDG2* along pseudo-time progression (Figure 7A and 7B). Analysis of the *SPCH*

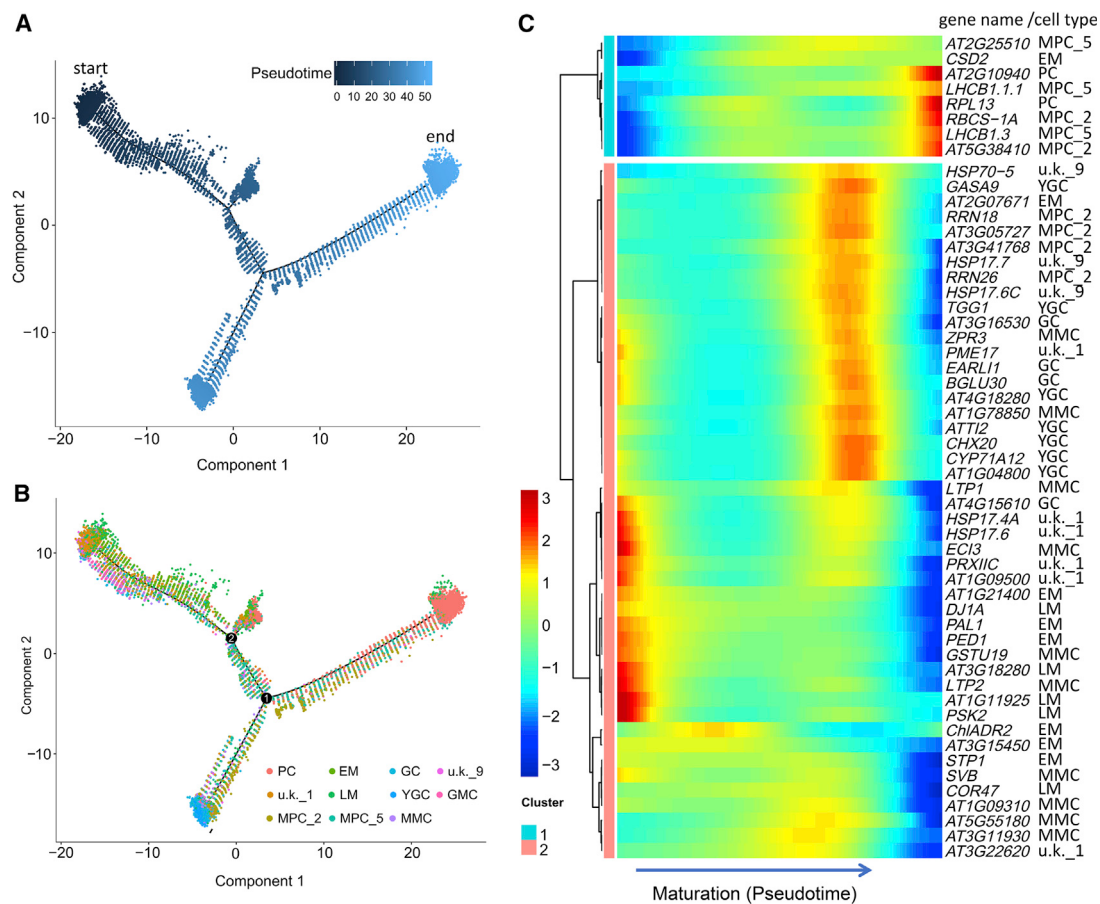


**Figure 6. Pseudo-Time Analysis of Clusters and Selected Marker Genes.**

(A) Distribution of cells in each cluster on the pseudo-time trajectory.

(B) Pseudo-time trajectory of single-cell transcriptomics data colored according to cluster. Most cells were distributed along the main stem, although two small branches were detected near the main path.

(C) Clustering and expression kinetics of representative genes along a pseudo-time progression of stomatal lineage cells. The name and cell type of marker genes are shown on the right of the heatmap.

chromatin immunoprecipitation sequencing (ChIP-seq) profile indicated that SPCH directly binds to the promoter regions of *ERL1*, *EPF1*, and *HDG2* (Figure 7C). Consistent with this, the expression levels of these genes in the *spch* mutant are lower than in WT (Figure 7D), raising the possibility that SPCH is involved in regulating the expression of its co-expressed genes along pseudo-time progression.

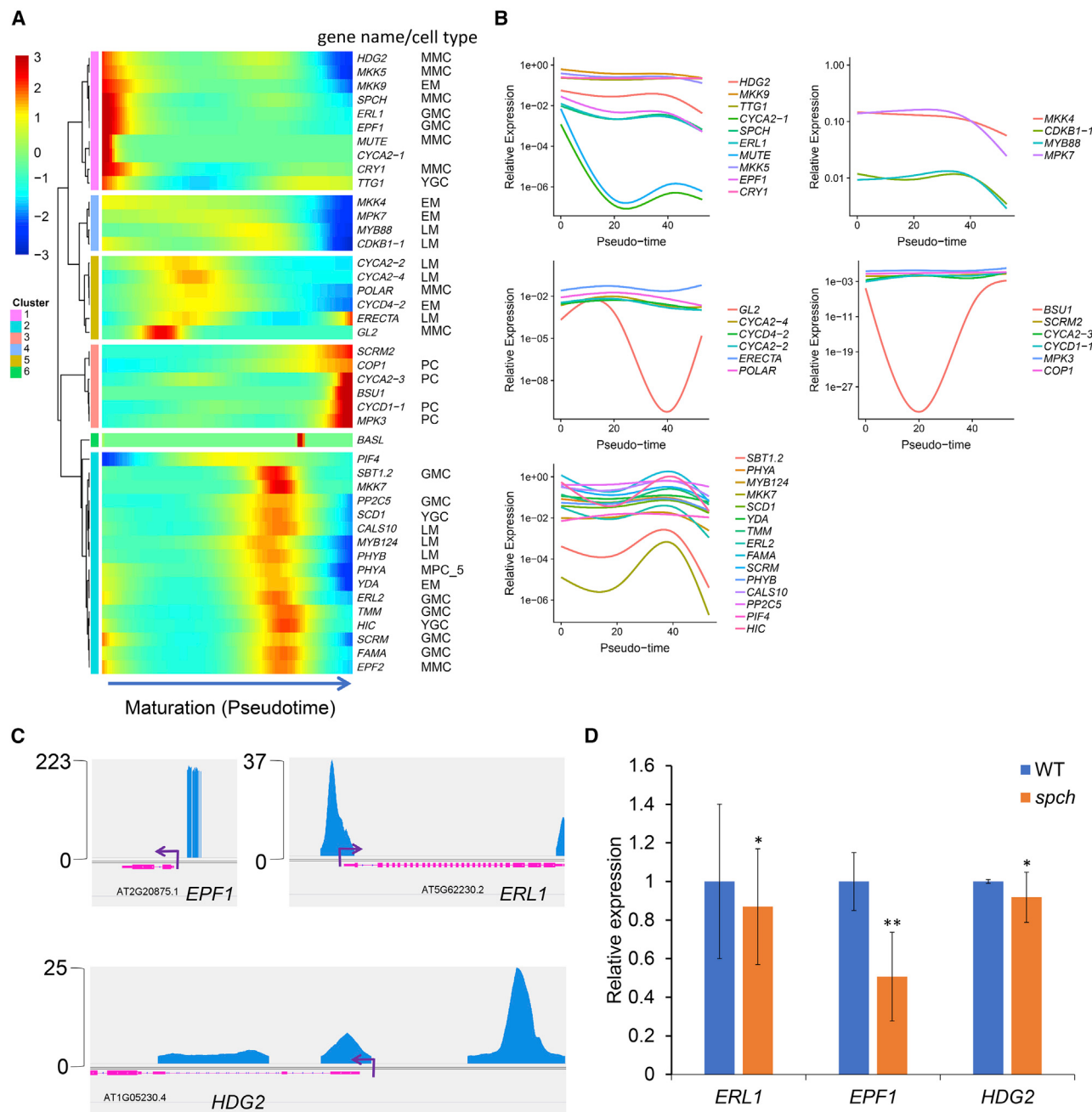
## DISCUSSION

Stomatal lineage cell fate decisions are traceable, irreversible, and produce well-known differentiated cell types. We were able to investigate the interplay of multiple fate-specific genetic programs and the effects of external environmental factors on the fate decisions of different cell types at the single-cell level. A combination of known marker genes and GO analysis enabled us to reliably classify and define cell types (Figure 1; Supplemental Figures 4 and 7). Transcripts of some marker genes (*SPCH*, *MUTE*, and *FAMA*) are enriched in specific types of stomatal lineage cells (Supplemental Figure 4) while those of other marker genes (*CRY1*, *PP2C*, *BCA4*, and *CALS10*) are not (Supplemental Figure 4). Furthermore, a series of new marker

genes were identified in different cell types (Figure 2). We also analyzed the effects of some marker genes on stomatal lineage cell development by checking the stomatal developmental patterns in the cotyledons of the corresponding mutants (Figures 4 and 5; Supplemental Figures 5 and 9).

## Determination of Cell Types and Marker Genes

The stomatal lineage cells can be classified into six different types—MMC, EM, LM, GMC, YGC, and GC—based on their developmental stages. To determine the cell type, we analyzed the feature plots of the expression of selected marker genes in specific cell types (Supplemental Figure 4B). We used more than one marker gene for identifying one cell type because marker genes are often expressed in more than one cell type and at different levels (Figure 1). MMCs, EMs, LMs, YGCs, and GCs can be clearly identified based on the existence of specific marker genes in each cluster. PCs contain chloroplasts and are difficult to distinguish from MPCs (Figure 1A). We could not determine the cell type of cluster 1 and cluster 9 using known marker genes (Figure 1A). Interestingly, we found that one marker gene from cluster 9, *BAG6*, may be involved in regulating the biogenesis of stomata based on the phenotype

**Figure 7. Pseudo-Time Analysis of Known Marker Genes.**

(A) Clustering of representative genes along a pseudo-time progression of stomatal lineage cells. The name and cell type of marker genes are shown on the right of the heatmap. The identification of cell type for CYCA2-1, SCRM2 and BSU1, BASL, PIF4, and MKK7 failed because their expression levels did not meet the criteria used to assign cell type.

(B) Gene expression kinetics along pseudo-time progression for representative genes.

(C) SPCH ChIP-seq profile of genes co-expressed with SPCH along pseudo-time progression. Scales for each track are shown on the left. Data are derived from Lau et al. (2014).

(D) Relative expression of genes in 5-day-old seedlings of the *spch* mutant and WT. Data are derived from Pillitteri et al. (2011). Error bars represent SE. \* $p < 0.05$ , \*\* $p < 0.01$ , Student's t-test analysis versus WT.

of a *bag6* mutant (Supplemental Figure 5). However, *bzip6*, the mutant of another marker gene of cluster 9, shows normal development of stomatal lineage cells (Supplemental Figure 5). The regulatory network mediated by SPCH has been characterized (Lau et al., 2014), and analysis of the target

genes of SPCH in all the clusters identified in this study indicates that the target genes are mainly enriched in MMCs (Supplemental Figure 11), consistent with the function of SPCH in the regulation of development of MMCs. These results further support the identification of MMCs in this study. We selected

the top 10 marker genes in each cluster as representative marker genes for the different cell types (Figure 2). Analysis of the marker genes in GCs indicates that some of them are involved in regulating the development and function of stomata (Figure 2A), suggesting that the marker genes identified can be used for determining the cell type.

### Potential Factors that Regulate the Fate of Stomatal Lineage Cells

Stomatal lineage cell development is regulated by many important factors, such as light, temperature, metabolism, and phytohormones (Pillitteri and Dong, 2013). In the past, most studies using cells from the whole plant could not clearly distinguish the specific functions of these factors in the different cell types. For instance, light signaling and hormone signaling can affect the entire process of stomatal lineage cell development (Pillitteri and Dong, 2013). Based on scRNA-seq combined with GO analysis, we were able to identify genes that potentially regulate stomatal lineage cell development. For example, GO heatmap analysis revealed that genes preferentially expressed in YGCs and GCs are mainly involved in the response to oxidative stress, abscisic acid, osmotic stress, and vacuolar activity (Supplemental Figures 7 and 8). The GO heatmap analysis also showed that GO terms enriched in MMCs, EMs, LMs, and GMCs are relatively similar (Supplemental Figures 7B and 8), suggesting that there are intense interactions among these cells in terms of gene expression and cell functions. It should be noted that genes highly expressed in MMCs are involved in the response to bacterial infection and in the MAPK signaling pathway (Supplemental Figures 7B and 8). Studies have shown that bacterial infection can generate a systemic signal that is translocated from the mature infected leaves to the developing leaves at the apical meristem, where it reduces stomatal density by increasing epidermal cell expansion (Dutton et al., 2019). After infections, fewer epidermal cells enter the stomatal lineage during the early stages of leaf development (Dutton et al., 2019). Taken together, our results indicate that genes expressed in MMCs may be involved in suppressing the biogenesis of stomatal cells in response to bacterial infection.

Analysis of the newly identified marker genes revealed that expression of *ATML1* and *PDF1* was specifically enhanced in MMCs. In addition, the expression levels of both *SPCH* and *MUTE* were decreased in *atml1-3* compared with WT (Supplemental Figure 9E). *ATML1* encodes a homeobox protein similar to *GL2* and is expressed in both the apical and basal daughter cells of the zygote as well as in its progeny cells (Peterson et al., 2013). Expression of *ATML1* starts at the two-cell stage of embryo development and is later restricted to the outermost epidermal cell layer (Iida et al., 2019). Overexpression of *ATML1* can induce the formation of stomata-like structures in the inner cells of the cotyledons in independent lines (Peterson et al., 2013). Therefore, taken together, these results suggest that *ATML1* can regulate the development of stomatal lineage cells by modulating the expression of both *SPCH* and *MUTE*.

### Involvement of a TF Regulatory Network in Regulating the Early-Stage Development of Stomatal Lineage Cells

It is well known that bHLH TFs play important roles in regulating stomatal lineage cell development (MacAlister et al., 2007;

Pillitteri et al., 2007). Recently, additional TFs that are involved in regulating stomatal lineage cell development have been identified, for example PIF4, MYB88, HDG2, and GL2 (Casson et al., 2009; Pillitteri and Dong, 2013). To identify additional TFs that regulate the development of specific cell types, we analyzed the TFs expressed in different stomatal lineage cells and found that *BPC1*, *BPC2*, *BPC4*, *BPC6*, and *WRKY33* are highly expressed in MMCs, EMs, and GMCs (Figure 3A and 3B). Analysis of the network of TFs indicated that PIF5, WRKY33, BPC1, and BPC6 may act as core TFs that regulate the differentiation from MMCs to GMCs (Figure 3C). The *BPC* gene family has seven members in *Arabidopsis* (Monfared et al., 2011). BPCs are GAGA binding proteins (GBPs), which bind GA-rich elements (Biggin and Tjian, 1988; Kooiker et al., 2005; Monfared et al., 2011) and are involved in regulating gene expression by interacting with chromatin remodeling complexes such as nucleosome remodeling factor and facilitating chromatin transcription (Lehmann, 2004). BPC TFs play important roles in regulating vegetative and reproductive development (Kooiker et al., 2005; Monfared et al., 2011; Simonini et al., 2012; Simonini and Kater, 2014; Mu et al., 2017; Shanks et al., 2018). Further analysis revealed that the stomatal density and SI in *wrky33* and in the *bpc* triple, quadruple, and sextuple mutants are different compared with those of WT, suggesting that these mutants are deficient in the regulation of stomatal lineage cell development (Figures 4 and 5). The expression levels of *SPCH*, *MUTE*, *FAMA*, *SCRM*, and *SCRM2* in the *bpc1 bpc2 bpc3 bpc4 bpc6 bpc7* sextuple mutant were lower than those in WT (Figure 5). These results suggest that BPCs may act as the core TFs that regulate the development of stomatal lineage cells.

### The Developmental Trajectory of Stomatal Lineage Cells

To dissect the temporal and spatial distribution of stomatal lineage cells, we performed a pseudo-time analysis of scRNA-seq data (Figures 6 and 7). As typical marker genes, *SPCH* and *MUTE* were found to be co-expressed with *EPF1*, *MKK5*, and *MKK9* (Figure 7A and 7B), suggesting that EPF1-MKK9/5-dependent signaling can influence both the expression and the function of *SPCH* and *MUTE*. More interestingly, light-signal receptor genes and stomatal lineage marker genes show strong co-expression patterns (Figure 7A). Different light-signal receptors rely on downstream COP1-YDA-MAPK signaling pathways to regulate different stages of stomatal lineage development in response to changes in light quality (Kang et al., 2009). Our results show that *SCRM2* and *COP1* exhibit very similar pseudo-time curves, while *SCRM* has the same pseudo-time curve as *PHYA* and *PHYB* (Figure 7A and 7B). The pseudo-time curve of the blue receptor *CRY1* is significantly different from those of *PHYA* and *PHYB* (Figure 7A and 7B). It has been reported that *EPF2* activates ER signaling, leading to subsequent MAPK activation and inhibition of stomatal lineage cell development, while *EPFL9* prevents *MPK3* and *MPK6* signal transduction (Lee et al., 2015). In the pseudo-time course, consistent with the regulatory relationships between *EPF2* and *MPK3*, we observed that the expression of *EPF2* preceded that of *MPK3* (Figure 7A and 7B).

The transition to GMCs is coordinated through cell-cycle controls and is promoted by *MUTE* (Han et al., 2018), while *FAMA* and

FLP/MYB88 act in parallel to antagonize the GMC transition (Lai et al., 2005). The canonical G<sub>1</sub> and G<sub>1</sub>/S-regulating CYCD family member CYCD5;1 is a MUTE target, implying that it may promote symmetric cell division commitment in an MUTE-dependent manner (Han et al., 2018). In addition to CYCD5;1, our results reveal that expression of CYCA2;1 is highly similar to that of MUTE and SPCH (Figure 7A and 7B). However, the expression of CYCA2;1 is restricted to the vascular tissues of leaves (Vanneste et al., 2011). The co-expression of MUTE and CYCA2;1 implies that the expression of these two genes can be induced at a similar development time, but the expression of CYCA2;1 may not be regulated by MUTE. The early-stage differentiation of stomatal lineage cells is complex and regulated by a regulatory circuit consisting of a positive feedback loop including SCRM/SCRM2 (SCRMs) and SPCH, and a negative feedback loop involving EPF2, TMM, and the SPCH●SCRMs module (Horst et al., 2015). Interestingly, as shown in Figure 7A, EPF2, TMM, and SCRM show highly similar profiles along pseudo-time while SPCH and SCRM2 show opposite profiles. The expression of SPCH decreases quickly from the start to the end of pseudo-time, but the expression of SCRM2 remains at a relatively low level and rapidly increases at the end of pseudo-time. On the contrary, expression of EPF2, TMM, and SCRM gradually increases in the early stage and reaches its highest level at the middle stage. The expression of these genes decreases to a very low level at the end of pseudo-time. Therefore, the expression patterns of these TFs along the pseudo-time course confirm the regulatory circuit identified by Horst et al. (2015).

## METHODS

### Screening and Verification of Mutants

T-DNA insertion mutants were obtained from the Arabidopsis Biological Resource Center (ABRC) (Supplemental Table 5). Mutant lines homozygous for the T-DNA insertion were identified by PCR analysis using gene-specific and T-DNA-specific primers (Supplemental Table 6 and Supplemental Figure 12). In addition, we also generated the BPC6-GFP transgenic lines.

### Constructs for Plant Transformation

To generate the pB7WGF2-BPC6 construct, we PCR-amplified the full-length cDNA of BPC6 using the primer pair presented in Supplemental Table 6. The PCR product was then purified, and first cloned into pDONR201 in a BP Clonase reaction (GATEWAY Cloning; Invitrogen) according to the manufacturer's instructions to generate pDONR-BPC6. The resulting plasmid was recombined into pB7WGF2 using LR Clonase (GATEWAY Cloning; Invitrogen) to generate the final construct.

### Plant Transformation

The pB7WGF2-BPC6 construct was transformed into *Agrobacterium tumefaciens* strain GV3105 via electroporation. The *A. tumefaciens* cells that contained pB7WGF2-BPC6 were then introduced into WT. The resulting T1 pB7WGF2-BPC6 transgenic plants were selected by BASTA as described previously (Sun et al., 2016). Homozygous transgenic plants were used in all experiments.

### Cotyledon Collection and Protoplast Preparation

We isolated protoplasts from cotyledons of 5-day-old *Arabidopsis* seedlings as described previously (Yoo et al., 2007) with slight modifications to adjust for the use cotyledon tissue. In brief, the cotyledons were harvested from seedlings and submerged in a solution (0.5 mM CaCl<sub>2</sub>, 0.5 mM MgCl<sub>2</sub>, 5 mM MES [2-(N-morpholino)ethanesulfonic acid], 1.5% Cellulase RS, 0.03% Pectolyase Y23, 0.25% BSA, 33 mg/l actinomycin

## Single-Cell RNA-Seq of Stomatal Lineage Cells

D, and 100 mg/l cordycepin [pH 5.5]) under vacuum for 10 min. The samples were then incubated for 4 h to isolate protoplasts. Thereafter, the isolated cells were washed three times with 8% mannitol buffer to remove Mg<sup>2+</sup>. Cells were then filtered with a 40-μm cell strainer. Cell activity was detected by trypan blue staining, and cell concentration was measured with a hemocytometer.

### Single-Cell RNA-Seq Library Preparation

We prepared scRNA-seq libraries with the Chromium Single Cell 3' Gel Beads-in-Emulsion Library & Gel Bead Kit v3 according to the user manual supplied by the kit.

### Single-Cell RNA-Seq Data Preprocessing

The Cell Ranger pipeline (version 3.0.0) provided by 10X Genomics was used to demultiplex cellular barcodes and map reads to the TAIR10 reference genome. Transcripts were quantified using the STAR aligner. We processed the unique molecular identifier (UMI) count matrix using the R package Seurat (version 2.3.4). To remove low-quality cells and likely multiple captures, we further applied criteria to filter out cells with UMI/gene numbers outside the limit of the mean value ± 2 standard deviations, assuming a Gaussian distribution for each cell's UMI/gene numbers. Following visual inspection of the distribution of cells by the fraction of chloroplast genes expressed, we further discarded low-quality cells where >40% of the counts belonged to chloroplast genes. After applying these quality control criteria, 12 844 single cells and 32 833 genes remained and were included in the downstream analyses. Library size normalization was performed in Seurat on the filtered matrix to obtain normalized counts.

Genes with the highest variable expression among single cells were identified using the method described previously (Macosko et al., 2015). In brief, the average expression and dispersion were calculated for all genes, which were subsequently placed into 11 bins based on expression. Principal component analysis (PCA) was performed to reduce the dimensionality on the log-transformed gene-barcode matrices of the most variable genes. Cells were clustered via a graph-based approach and visualized in two dimensions using tSNE. A likelihood ratio test, which simultaneously tests for changes in mean expression and percentage of cells expressing a gene, was used to identify significantly differentially expressed genes (DEGs) between clusters. We also performed tSNE analyses and identified the DEGs between clusters for the mesophyll and stomatal lineage cell populations.

To confirm the cell clusters identified by tSNE, we also performed UMAP analysis (Becht et al., 2019). For PCA, the scaled data were reduced into 30 approximate principal components depending on 5965 highly variable genes (set nprcs = 30). Clusters were identified using the Seurat function 'FindClusters' with "resolution = 0.4". The data structures were separately visualized and explored by UMAP (by running the 'RunUMAP' function with "n.neighbors = 30, metric = correlation and min.dist = 0.3").

Pseudo-time trajectory analysis of single-cell transcriptomes was conducted using Monocle 2 (Trapnell et al., 2014). For pseudo-time analysis, the raw count in the Seurat object was first converted into the CellDataSet with the importCDS (object, import\_all = F) function in Monocle 2. We then used the estimateSizeFactors() and estimateDispersions() functions to pre-calculate some parameters. Specifically, size factors helped us to normalize the differences in mRNA recovered across cells, and "dispersion" values helped us to perform the differential expression analysis later. We used the differentialGeneTest function (fullModelFormulaStr = "clusters") of the Monocle 2 package for ordering genes (qval < 0.01) that were likely to be informative for ordering cells along the pseudo-time trajectory. The ordered genes were then marked with the setOrderingFilter() function. The dimensional reduction clustering analysis was performed with the reduceDimension() function, max\_components = 2, reduction\_method = "DDRTree", then

with the trajectory inference ('orderCells' function) with default parameters. Gene expression was then plotted as a function of pseudo-time in Monocle 2 to track changes across pseudo-time. We also plotted TFs and marker genes along the inferred developmental pseudo-time.

The regulation networks for the TFs and target genes were plotted by Cytoscape according to the PlantTFDB database. Bulk and single-cell RNA-seq correlation analysis was performed as described by Rheaume et al. (2018). Differential expression analysis was performed with *t*-test. Using the *t*.test function to test the differences in gene expression value between scRNA-seq and bulk RNA-seq, a significant *p* value was obtained. The difference multiple of  $\log_2$  fold change (FC) was calculated as follows:  $\log_2((\text{mean gene expression value in scRNA-seq}) + 0.001) / ((\text{mean gene expression value in bulk RNA-seq}) + 0.001)$ . Finally, the genes with significant differences in expression between samples were identified according to *p* value <0.05 and  $|\log_2\text{FC}| > 1$ .

### RNA-Seq Analysis

Cotyledons of 5-day-old seedlings were harvested for extracting total RNA using the mirVana miRNA Isolation Kit (Ambion) following the manufacturer's protocol. The samples with RNA Integrity Number (RIN)  $\geq 7$  were subjected to subsequent RNA-seq analysis. The libraries were constructed using the TruSeq Stranded mRNA LTSample Prep Kit (Illumina, San Diego, CA, USA) according to the manufacturer's instructions. Libraries were sequenced on the Illumina sequencing platform (HiSeq 2500 or Illumina HiSeq X Ten) and 125-bp/150-bp paired-end reads were generated.

### Microscopy

The cotyledons were observed 5 days after germination. The samples were harvested and placed in 70% ethanol, cleared overnight at room temperature, and stored in Hoyer's solution. Images of stomata were obtained from samples stored in Hoyer's solution and visualized using differential interference contrast microscopy with a Leica DMI8 microscope. A Nikon D-ECLIPSE C1 laser confocal scanning microscope was used for GFP images.

### Gene Ontology Enrichment Analysis

The enrichment of GO terms and pathways for the DEGs were analyzed using Metascape (<http://metascape.org/>) (Zhou et al., 2019).

### ACCESSION NUMBERS

Sequence data from this study can be found in the *Arabidopsis* Genome Initiative data library under the following accession numbers: WRKY33 (AT1G07890), BPC1 (AT2G01930), BPC2 (AT1G14685), BPC3 (AT1G68120), BPC4 (AT2G21240), BPC6 (AT5G42520), BPC7 (AT2G35550), ATML1 (AT4G21750), BAG6 (AT2G46240), bZIP6 (AT2G22850). scRNA-seq data are available at [https://www.ncbi.nlm.nih.gov/sra?LinkName=biosample\\_sra&from\\_uid=14069740](https://www.ncbi.nlm.nih.gov/sra?LinkName=biosample_sra&from_uid=14069740).

### SUPPLEMENTAL INFORMATION

Supplementary Information is available at *Molecular Plant Online*.

### FUNDING

This research was supported by the National Natural Science Foundation of China (31670233) and the Key Scientific and Technological Projects in Henan Province, China (192102110113).

### AUTHOR CONTRIBUTIONS

X.S. designed the study; Z.L., Y.Z., J.G., Z.Z., J.L., Z.T., J.W., R.W., B.Z., W.L., T.L., Yonjian Hu, and Yunhe Hu performed the research; J.-D.R., Y.M., and X.S. analyzed the data; X.S. and J.-D.R. wrote the paper. All authors discussed the results and made comments on the manuscript.

### ACKNOWLEDGMENTS

We are grateful to ABRC for the *Arabidopsis* seeds. We thank Prof. Charles Gasser for providing the *bpc double*, *triple*, *quadruple*, and *sextuple* mutant seeds. We thank Dr. Yunping Xiao, Dr. Yao Lu, and Dr. Yongbing Ba for help in data processing. No conflict of interest declared.

Received: March 25, 2020

Revised: April 26, 2020

Accepted: June 22, 2020

Published: June 24, 2020

### REFERENCES

- Adrian, J., Chang, J., Ballenger, C.E., Bargmann, B.O.R., Alassimone, J., Davies, K.A., Lau, O.S., Matos, J.L., Hachez, C., Lanctot, A., et al. (2015). Transcriptome dynamics of the stomatal lineage: birth, amplification, and termination of a self-renewing population. *Dev. Cell* **33**:107–118.
- Amsbury, S., Hunt, L., Elhaddad, N., Baillie, A., Lundgren, M., Verhertbruggen, Y., Scheller, H.V., Knox, J.P., Fleming, A.J., and Gray, J.E. (2016). Stomatal function requires pectin de-methyl-esterification of the guard cell wall. *Curr. Biol.* **26**:2899–2906.
- Barton, K.A., Schattat, M.H., Jakob, T., Hause, G., Wilhelm, C., McKenna, J.F., Mathe, C., Runions, J., Van Damme, D., and Mathur, J. (2016). Epidermal pavement cells of *Arabidopsis* have chloroplasts. *Plant Physiol.* **171**:723–726.
- Becht, E., McInnes, L., Healy, J., Dutertre, C.A., Kwok, I.W.H., Ng, L.G., Ginhoux, F., and Newell, E.W. (2019). Dimensionality reduction for visualizing single-cell data using UMAP. *Nat. Biotechnol.* **37**:38.
- Bergmann, D.C., Lukowitz, W., and Somerville, C.R. (2004). Stomatal development and pattern controlled by a MAPKK kinase. *Science* **304**:1494–1497.
- Bergmann, D.C., and Sack, F.D. (2007). Stomatal development. *Annu. Rev. Plant Biol.* **58**:163–181.
- Biggin, M.D., and Tjian, R. (1988). Transcription factors that activate the Ultrabithorax promoter in developmentally staged extracts. *Cell* **53**:699–711.
- Casson, S.A., Franklin, K.A., Gray, J.E., Grierson, C.S., Whitelam, G.C., and Hetherington, A.M. (2009). phytochrome B and PIF4 regulate stomatal development in response to light quantity. *Curr. Biol.* **19**:229–234.
- Chen, L., Guan, L.P., Qian, P.P., Xu, F., Wu, Z.L., Wu, Y.J., He, K., Gou, X.P., Li, J., and Hou, S.W. (2016). NRPB3, the third largest subunit of RNA polymerase II, is essential for stomatal patterning and differentiation in *Arabidopsis*. *Development* **143**:1600–1611.
- Denyer, T., Ma, X., Klesen, S., Scacchi, E., Nieselt, K., and Timmermans, M.C.P. (2019). Spatiotemporal developmental trajectories in the *Arabidopsis* root revealed using high-throughput single-cell RNA sequencing. *Dev. Cell* **48**:840–852 e845.
- Dong, J., MacAlister, C.A., and Bergmann, D.C. (2009). BASL controls asymmetric cell division in *Arabidopsis*. *Cell* **137**:1320–1330.
- Dutton, C., Horak, H., Hepworth, C., Mitchell, A., Ton, J., Hunt, L., and Gray, J.E. (2019). Bacterial infection systemically suppresses stomatal density. *Plant Cell Environ.* **42**:2411–2421.
- Engineer, C.B., Ghassemian, M., Anderson, J.C., Peck, S.C., Hu, H.H., and Schroeder, J.I. (2015). Carbonic anhydrases, EPF2 and a novel protease mediate CO<sub>2</sub> control of stomatal development (vol 513, pg 246, 2014). *Nature* **526**:458.
- Geisler, M., Nadeau, J., and Sack, F.D. (2000). Oriented asymmetric divisions that generate the stomatal spacing pattern in *Arabidopsis* are disrupted by the too many mouths mutation. *Plant Cell* **12**:2075–2086.
- Gray, J. (2005). Guard cells: transcription factors regulate stomatal movements. *Curr. Biol.* **15**:R593–R595.

- Gray, J.E., Holroyd, G.H., van der Lee, F.M., Bahrami, A.R., Sijmons, P.C., Woodward, F.I., Schuch, W., and Heterington, A.M.** (2000). The HIC signalling pathway links CO<sub>2</sub> perception to stomatal development. *Nature* **408**:713–716.
- Han, S.K., Qi, X., Sugihara, K., Dang, J.H., Endo, T.A., Miller, K.L., Kim, E.D., Miura, T., and Torii, K.U.** (2018). MUTE directly orchestrates cell-state switch and the single symmetric division to create stomata. *Dev. Cell* **45**:303–315 e305.
- Han, S.K., and Torii, K.U.** (2016). Lineage-specific stem cells, signals and asymmetries during stomatal development. *Development* **143**:1259–1270.
- Hara, K., Kajita, R., Torii, K.U., Bergmann, D.C., and Kakimoto, T.** (2007). The secretory peptide gene EPF1 enforces the stomatal one-cell-spacing rule. *Gene Dev.* **21**:1720–1725.
- Horst, R.J., Fujita, H., Lee, J.S., Rychel, A.L., Garrick, J.M., Kawaguchi, M., Peterson, K.M., and Torii, K.U.** (2015). Molecular framework of a regulatory circuit initiating two-dimensional spatial patterning of stomatal lineage. *PLoS Genet.* **11**:e1005374.
- Houbaert, A., Zhang, C., Tiwari, M., Wang, K., de Marcos Serrano, A., Savatin, D.V., Urs, M.J., Zhiponova, M.K., Gudesblat, G.E., Vanhoutte, I., et al.** (2018). POLAR-guided signalling complex assembly and localization drive asymmetric cell division. *Nature* **563**:574–578.
- Hronkova, M., Wiesnerova, D., Simkova, M., Skupa, P., Dewitte, W., Vrablova, M., Zazimalova, E., and Santrucek, J.** (2015). Light-induced STOMAGEN-mediated stomatal development in *Arabidopsis* leaves. *J. Exp. Bot.* **66**:4621–4630.
- Huang, S., Waadt, R., Nuhkat, M., Kollist, H., Hedrich, R., and Roelfsema, M.R.G.** (2019). Calcium signals in guard cells enhance the efficiency by which ABA triggers stomatal closure. *New Phytol.* **224**:177–187.
- Hunt, L., and Gray, J.E.** (2009a). The signaling peptide EPF2 controls asymmetric cell divisions during stomatal development. *Curr. Biol.* **19**:864–869.
- Hunt, L., and Gray, J.E.** (2009b). The signaling peptide EPF2 controls asymmetric cell divisions during stomatal development. *Curr. Biol.* **19**:864–869.
- Iida, H., Yoshida, A., and Takada, S.** (2019). ATML1 activity is restricted to the outermost cells of the embryo through post-transcriptional repressions. *Development* **146**:dev169300.
- Jean-Baptiste, K., McFaline-Figueroa, J.L., Alexandre, C.M., Dorrrity, M.W., Saunders, L., Bubb, K.L., Trapnell, C., Fields, S., Queitsch, C., and Cuperus, J.T.** (2019). Dynamics of gene expression in single root cells of *Arabidopsis thaliana*. *Plant Cell* **31**:993–1011.
- Kanaoka, M.M., Pillitteri, L.J., Fujii, H., Yoshida, Y., Bogenschutz, N.L., Takabayashi, J., Zhu, J.K., and Torii, K.U.** (2008). SCREAM/ICE1 and SCREAM2 specify three cell-state transitional steps leading to *Arabidopsis* stomatal differentiation. *Plant Cell* **20**:1775–1785.
- Kang, C.Y., Lian, H.L., Wang, F.F., Huang, J.R., and Yang, H.Q.** (2009). Cryptochromes, phytochromes, and COP1 regulate light-controlled stomatal development in *Arabidopsis*. *Plant Cell* **21**:2624–2641.
- Kim, T.W., Michniewicz, M., Bergmann, D.C., and Wang, Z.Y.** (2012). Brassinosteroid regulates stomatal development by GSK3-mediated inhibition of a MAPK pathway. *Nature* **482**:419–U1526.
- Kooiker, M., Aioldi, C.A., Losa, A., Manzotti, P.S., Finzi, L., Kater, M.M., and Colombo, L.** (2005). BASIC PENTACysteine1, a GA binding protein that induces conformational changes in the regulatory region of the homeotic *Arabidopsis* gene SEEDSTICK. *Plant Cell* **17**:722–729.
- Lai, L.B., Nadeau, J.A., Lucas, J., Lee, E.K., Nakagawa, T., Zhao, L.M., Geisler, M., and Sack, F.D.** (2005). The *Arabidopsis* R2R3 MYB proteins FOUR LIPS and MYB88 restrict divisions late in the stomatal cell lineage. *Plant Cell* **17**:2754–2767.
- Lampard, G.R., MacAlister, C.A., and Bergmann, D.C.** (2008). *Arabidopsis* stomatal initiation is controlled by MAPK-mediated regulation of the bHLH SPEECHLESS. *Science* **322**:1113–1116.
- Lampard, G.R., Lukowitz, W., Ellis, B.E., and Bergmann, D.C.** (2009). Novel and expanded roles for MAPK signaling in *Arabidopsis* stomatal cell fate revealed by cell type-specific manipulations. *Plant Cell* **21**:3506–3517.
- Lau, O.S., Davies, K.A., Chang, J., Adrian, J., Rowe, M.H., Ballenger, C.E., and Bergmann, D.C.** (2014). Direct roles of SPEECHLESS in the specification of stomatal self-renewing cells. *Science* **345**:1605–1609.
- Lawson, T.** (2009). Guard cell photosynthesis and stomatal function. *New Phytol.* **181**:13–34.
- Lee, J.S., Kuroha, T., Hnilova, M., Khatayevich, D., Kanaoka, M.M., McAbee, J.M., Sarikaya, M., Tamerler, C., and Torii, K.U.** (2012). Direct interaction of ligand-receptor pairs specifying stomatal patterning. *Gene Dev.* **26**:126–136.
- Lee, J.S., Hnilova, M., Maes, M., Lin, Y.C.L., Putarjunan, A., Han, S.K., Avila, J., and Torii, K.U.** (2015). Competitive binding of antagonistic peptides fine-tunes stomatal patterning. *Nature* **522**:435.
- Lehmann, M.** (2004). Anything else but GAGA: a nonhistone protein complex reshapes chromatin structure. *Trends Genet.* **20**:15–22.
- Liang, H., Zhang, Y., Martinez, P., Rasmussen, C.G., Xu, T., and Yang, Z.** (2018). The microtubule-associated protein IQ67 DOMAIN5 modulates microtubule dynamics and pavement cell shape. *Plant Physiol.* **177**:1555–1568.
- Liu, L., Lin, N., Liu, X., Yang, S., Wang, W., and Wan, X.** (2020). From chloroplast biogenesis to chlorophyll accumulation: the interplay of light and hormones on gene expression in camellia sinensis cv. Shuchazao leaves. *Front. Plant Sci.* **11**:256.
- MacAlister, C.A., Ohashi-Ito, K., and Bergmann, D.C.** (2007). Transcription factor control of asymmetric cell divisions that establish the stomatal lineage. *Nature* **445**:537–540.
- Macosko, E.Z., Basu, A., Satija, R., Nemesh, J., Shekhar, K., Goldman, M., Tirosh, I., Bialas, A.R., Kamitaki, N., Martersteck, E.M., et al.** (2015). Highly parallel genome-wide expression profiling of individual cells using nanoliter droplets. *Cell* **161**:1202–1214.
- Monfared, M.M., Simon, M.K., Meister, R.J., Roig-Villanova, I., Kooiker, M., Colombo, L., Fletcher, J.C., and Gasser, C.S.** (2011). Overlapping and antagonistic activities of BASIC PENTACysteine genes affect a range of developmental processes in *Arabidopsis*. *Plant J.* **66**:1020–1031.
- Mu, Y., Zou, M., Sun, X., He, B., Xu, X., Liu, Y., Zhang, L., and Chi, W.** (2017). BASIC PENTACysteine proteins repress ABSCISIC ACID INSENSITIVE4 expression via direct recruitment of the polycomb-repressive complex 2 in *Arabidopsis* root development. *Plant Cell Physiol.* **58**:607–621.
- Nadeau, J.A., and Sack, F.D.** (2002). Control of stomatal distribution on the *Arabidopsis* leaf surface. *Science* **296**:1697–1700.
- Niu, M.L., Huang, Y., Sun, S.T., Sun, J.Y., Cao, H.S., Shabala, S., and Bie, Z.L.** (2018). Root respiratory burst oxidase homologue-dependent H<sub>2</sub>O<sub>2</sub> production confers salt tolerance on a grafted cucumber by controlling Na<sup>+</sup> exclusion and stomatal closure. *J. Exp. Bot.* **69**:3465–3476.
- Ohashi-Ito, K., and Bergmann, D.C.** (2006). *Arabidopsis* FAMA controls the final proliferation/differentiation switch during stomatal development. *Plant Cell* **18**:2493–2505.
- Peterson, K.M., Shyu, C., Burr, C.A., Horst, R.J., Kanaoka, M.M., Omae, M., Sato, Y., and Torii, K.U.** (2013). *Arabidopsis*

## Single-Cell RNA-Seq of Stomatal Lineage Cells

homeodomain-leucine zipper IV proteins promote stomatal development and ectopically induce stomata beyond the epidermis. *Development* **140**:1924–1935.

**Pillitteri, L.J., and Dong, J.** (2013). Stomatal development in *Arabidopsis*. *Arabidopsis Book* **11**:e0162.

**Pillitteri, L.J., and Torii, K.U.** (2012). Mechanisms of stomatal development. *Annu. Rev. Plant Biol.* **63**:591–614.

**Pillitteri, L.J., Sloan, D.B., Bogenschutz, N.L., and Torii, K.U.** (2007). Termination of asymmetric cell division and differentiation of stomata. *Nature* **445**:501–505.

**Pillitteri, L.J., Peterson, K.M., Horst, R.J., and Torii, K.U.** (2011). Molecular profiling of stomatal meristemoids reveals new component of asymmetric cell division and commonalities among stem cell populations in *Arabidopsis*. *Plant Cell* **23**:3260–3275.

**Putarjunan, A., Ruble, J., Srivastava, A., Zhao, C., Rychel, A.L., Hofstetter, A.K., Tang, X., Zhu, J.K., Tama, F., Zheng, N., et al.** (2019). Bipartite anchoring of SCREAM enforces stomatal initiation by coupling MAP kinases to SPEECHLESS. *Nat. Plants* **5**:742–754.

**Qu, X., Peterson, K.M., and Torii, K.U.** (2017). Stomatal development in time: the past and the future. *Curr. Opin. Genet. Dev.* **45**:1–9.

**Rheaume, B.A., Jereen, A., Bolisetty, M., Sajid, M.S., Yang, Y., Renna, K., Sun, L., Robson, P., and Trakhtenberg, E.F.** (2018). Single cell transcriptome profiling of retinal ganglion cells identifies cellular subtypes. *Nat. Commun.* **9**:2759.

**Rudall, P.J., Hilton, J., and Bateman, R.M.** (2013). Several developmental and morphogenetic factors govern the evolution of stomatal patterning in land plants. *New Phytol.* **200**:598–614.

**Ryu, K.H., Huang, L., Kang, H.M., and Schiefelbein, J.** (2019). Single-cell RNA sequencing resolves molecular relationships among individual plant cells. *Plant Physiol.* **179**:1444–1456.

**Salesse, C., Sharwood, R., Sakamoto, W., and Stern, D.** (2017). The rubisco chaperone BSD2 may regulate chloroplast coverage in maize bundle sheath cells. *Plant Physiol.* **175**:1624–1633.

**Samakovli, D., Ticha, T., Vavrdova, T., Ovecka, M., Luptovciak, I., Zapletalova, V., Kucharova, A., Krenek, P., Krasylenko, Y., Margaritopoulou, T., et al.** (2020). YODA-HSP90 module regulates phosphorylation-dependent inactivation of SPEECHLESS to control stomatal development under acute heat stress in *Arabidopsis*. *Mol. Plant* **13**:612–633.

**Schmidt, A., Machtel, R., Ammon, A., Engelsdorf, T., Schmitz, J., Maurino, V.G., and Voll, L.M.** (2020). Reactive oxygen species dosage in *Arabidopsis* chloroplasts can improve resistance towards *Colletotrichum higginsianum* by the induction of WRKY33. *New Phytol.* **226**:189–204.

**Shanks, C.M., Hecker, A., Cheng, C.Y., Brand, L., Collani, S., Schmid, M., Schaller, G.E., Wanke, D., Harter, K., and Kieber, J.J.** (2018). Role of BASIC PENTACysteine transcription factors in a subset of cytokinin signaling responses. *Plant J.* **95**:458–473.

**Shpak, E.D., McAbee, J.M., Pillitteri, L.J., and Torii, K.U.** (2005). Stomatal patterning and differentiation by synergistic interactions of receptor kinases. *Science* **309**:290–293.

**Simonini, S., and Kater, M.M.** (2014). Class I BASIC PENTACysteine factors regulate HOMEobox genes involved in meristem size maintenance. *J. Exp. Bot.* **65**:1455–1465.

## Molecular Plant

**Simonini, S., Roig-Villanova, I., Gregis, V., Colombo, B., Colombo, L., and Kater, M.M.** (2012). Basic pentacysteine proteins mediate MADS domain complex binding to the DNA for tissue-specific expression of target genes in *Arabidopsis*. *Plant Cell* **24**:4163–4172.

**Song, Y., Miao, Y., and Song, C.P.** (2014). Behind the scenes: the roles of reactive oxygen species in guard cells. *New Phytol.* **201**:1121–1140.

**Sugano, S.S., Shimada, T., Imai, Y., Okawa, K., Tamai, A., Mori, M., and Hara-Nishimura, I.** (2010). Stomagen positively regulates stomatal density in *Arabidopsis*. *Nature* **463**:241–244.

**Sun, X., Xu, D., Liu, Z., Kleine, T., and Leister, D.** (2016). Functional relationship between mTERF4 and GUN1 in retrograde signaling. *J. Exp. Bot.* **67**:3909–3924.

**Takada, S., Takada, N., and Yoshida, A.** (2013). ATML1 promotes epidermal cell differentiation in *Arabidopsis* shoots. *Development* **140**:1919–1923.

**Trapnell, C., Cacchiarelli, D., Grimsby, J., Pokharel, P., Li, S., Morse, M., Lennon, N.J., Livak, K.J., Mikkelsen, T.S., and Rinn, J.L.** (2014). The dynamics and regulators of cell fate decisions are revealed by pseudotemporal ordering of single cells. *Nat. Biotechnol.* **32**:381–386.

**Vanneste, S., Coppens, F., Lee, E., Donner, T.J., Xie, Z., Van Isterdael, G., Dhondt, S., De Winter, F., De Rybel, B., Vuylsteke, M., et al.** (2011). Developmental regulation of CYCA2s contributes to tissue-specific proliferation in *Arabidopsis*. *EMBO J.* **30**:3430–3441.

**von Groll, U., and Altmann, T.** (2001). Stomatal cell biology. *Curr. Opin. Plant Biol.* **4**:555–560.

**Wang, Y., Schuck, S., Wu, J., Yang, P., Doring, A.C., Zeier, J., and Tsuda, K.** (2018). A MPK3/6-WRKY33-ALD1-pipeolic acid regulatory loop contributes to systemic acquired resistance. *Plant Cell* **30**:2480–2494.

**Xue, X., Bian, C., Guo, X., Di, R., and Dong, J.** (2020). The MAPK substrate MASS proteins regulate stomatal development in *Arabidopsis*. *PLoS Genet.* **16**:e1008706.

**Yang, Y., Costa, A., Leonhardt, N., Siegel, R.S., and Schroeder, J.I.** (2008). Isolation of a strong *Arabidopsis* guard cell promoter and its potential as a research tool. *Plant Methods* **4**:6.

**Yang, K.Z., Jiang, M., Wang, M., Xue, S., Zhu, L.L., Wang, H.Z., Zou, J.J., Lee, E.K., Sack, F., and Le, J.** (2015). Phosphorylation of serine 186 of bHLH transcription factor SPEECHLESS promotes stomatal development in *Arabidopsis*. *Mol. Plant* **8**:783–795.

**Yoo, S.D., Cho, Y.H., and Sheen, J.** (2007). *Arabidopsis* mesophyll protoplasts: a versatile cell system for transient gene expression analysis. *Nat. Protoc.* **2**:1565–1572.

**Zhang, J.Y., He, S.B., Li, L., and Yang, H.Q.** (2014). Auxin inhibits stomatal development through MONOPTEROS repression of a mobile peptide gene STOMAGEN in mesophyll. *Proc. Natl. Acad. Sci. U S A* **111**:E3015–E3023.

**Zhang, T.Q., Xu, Z.G., Shang, G.D., and Wang, J.W.** (2019). A single-cell RNA sequencing profiles the developmental landscape of *Arabidopsis* root. *Mol. Plant* **12**:648–660.

**Zhou, Y., Zhou, B., Pache, L., Chang, M., Khodabakhshi, A.H., Tanaseichuk, O., Benner, C., and Chanda, S.K.** (2019). Metascape provides a biologist-oriented resource for the analysis of systems-level datasets. *Nat. Commun.* **10**:1523.